ELSEVIER

Contents lists available at ScienceDirect

Composites Part B

journal homepage: www.elsevier.com/locate/compositesb





Synthesis of carbon from waste coconutshell and their application as filler in bioplast polymer filaments for 3D printing

Chibu O. Umerah, Deepa Kodali, Sydnei Head, Shaik Jeelani, Vijaya K. Rangari a

Department of Materials Science and Engineering, Tuskegee University, Tuskegee, AL, 36088, USA

ARTICLE INFO

Keywords:
Coconut shell powder
3D printing
Polymer biocomposite

ABSTRACT

Environmental friendly plastics offer suitable alternatives to the hazardous non-degradable plastics. In this work, we explored biodegradable plastic created from BIOPLAST GF 106/02/PLA 75/25 blend (BPB) with carbon nanoparticles (CCSP10) derived from waste coconut shell. The CCSP nanoparticles were synthesized using high temperature/pressure reactor and characterized using analytical tools such as Scanning electron microscopy (SEM), X-ray diffraction (XRD), and Raman spectroscopy to investigate the properties of as prepared carbon nanoparticles. The neat BIOPLAST GF 106/02 (BP) polymer and carbon infused BP polymer composite filaments were created from solvent based blending and extruded into filaments. The filament specimens were then characterized using thermogravimetric analysis (TGA), differential scanning calorimetric (DSC), tensile and electrical conductivity tests. The influence of extrusion and monodispersed size reduced particles have potentially increased the mechanical strength by altering the structure of the polymer blends. The polymer composite filaments of BPB infused with 0.2 wt %, 0.6 wt %, and 1 wt % carbon nanoparticles show increased mechanical strength. The tensile strength increased by 50% compared to neat BP filaments with the increase in carbon nanoparticles content up to 0.6 wt% and then decreased due to agglomeration of particles. TGA showed that the presence of CCSP resulted in additional decomposition and decreased weight loss. The electrical conductivity tests proved that increasing the filler content increased the conductivity. These filaments are designed for 3D printing of polymer composite applications.

1. Introduction

3D printing of biodegradable filaments has become subject of interest for researchers in the field of extrusion of polymer nanocomposites due to their wide variety of applications and advantages [1–6]. The biocomposite materials decrease the need for synthetic polymers and thus contribute to subside the environmental pollution [2, 7]. Most biocomposites are made up of natural fillers obtained from widely available agricultural and industrial wastes resulting in low density materials at low cost with agreeable mechanical properties [8]. Although the research on biodegradable 3D printable filaments is trending, the need for the biodegradable composites is nevertheless increasing to meet the demand of the diverse requirements of the industries [9].

Biocarbon which is also known as biochar being emerged as a new sustainable material has attracted the attention of researchers for various commercial applications [10]. In addition to the application as filler reinforcement, biochar is also advantageous to generate carbon

based next generation functional materials [11]. However, in view of the applications based on biochar reinforced biopolymer composites, the studies reported were limited [12]. The biochar from the landfill pine wood waste was used to develop polypropylene-based composites which have shown beneficial flame retardant behavior [13]. The silica produced from bagasse ash was used as a filler for Bioplast GF106/02 resulting in improved mechanical and thermal properties of the composites [14]. Remarkably, the bio-char from the packaging waste was melt mixed with poly (ethylene terephthalate) to generate 3D printable filaments [15]. The 3D printed parts have shown enhanced mechanical, thermal and dynamic properties. The biochar from bamboo charcoal was used to develop electrically conductive ultra-high molecular weight polyethylene composites [16]. Similarly, Biochar from bamboo charcoal has improved tensile strength, flexural strength and ductility index when used as reinforcement for polylactic acid (PLA) [17]. Rice husk hydrochar infused PLA composites have shown improved mechanical properties. In view of these advantages, and based on the wide availability of agro based waste, this study focused on developing

E-mail address: vrangari@tuskegee.edu (V.K. Rangari).

^{*} Corresponding author.

biodegradable filaments for 3D printing applications.

Coconut shell (CS) is an agro waste which is available in ample volume worldwide. Predominantly, India, Indonesia, Philippines, and Sri Lanka are the leading producers of coconuts. The coconut shell waste is underutilized and is burnt in the open air or disposed in the ponds resulting in environmental pollution [7,18]. Owing to its chemical composition, CS fiber proved to be potential candidate for the enhancement of new composites for their high strength and modulus properties [2,19]. Coconut shell consists of cellulose (26.6%), hemicellulose (21%), lignin (29.4%), pentosans (27.7%), solvent extractives (4.2%), uronic anhydrides (3.5%), and ash (0.6%) [7]. Elementally, coconut shell has a high content of carbon (49.86%) and is efficiently used to produce charcoal and activated carbon [18]. Activated carbon from coconut shell is often used as adsorbent due to high porosity and surface area [20,21]. Being ecofriendly and biodegradable, carbon from coconut shell has been heavily used for current polymer technology to serve as an alternative filler for synthetic materials [22]. This will result in less dependency on non-biodegradable polymers, thus creating a safer material. Carbon from coconut shell often serves as a filler for thermosets like epoxy resin and thermoplastics including polypropylene to increase its biodegradability [23–25]. Thermoplastics such as polylactic acid (PLA) are used as the matrix for the polymer composites, and carbon derived from coconut shell serves as its filler in order to make a completely biodegradable material [26].

Polylactic acid (PLA) is one of the most widely used biopolymers for commercial applications. PLA is produced from renewable resources like corn by polymerization, which causes the ring of the lactide monomer to open or through polycondensation reaction [27,28]. This can be challenging to obtain PLA with a high molecular weight due to water being formed during the polycondensation reaction. An alternative route would consist of pre-polymer lactide dimers with low molecular weight being formed during condensation, with the second step causing the pre-polymers to change into a PLA with high molecular weight through ring-opening polymerization with specific catalysts [28].

However, to the best of our knowledge, there were no studies reported on bio-based polymer, BIOPLAST GF 106/02 (BP) infused with carbon from coconut shell powder. BIOPLAST GF 106/02 (BP) is a thermoplastic material that is plasticizer-free, GMO-free, and contains 23% of bio-based and content which is natural potato starch [29]. This material is suitable for processes such as blown film extrusion to produce completely biodegradable and biorenewable products. When plasticizer is absent, BP can be processed to manufacture lasting products of dependable quality with ease. The shell life of the material is excellent; however, it will biodegrade after service life in an industrial composting environment. General applications for this material include; short life packaging, multi-use bags (e.g. carrier bags, loop-handle bags), single-use bags (e.g. refuse bags, bin liners), food packaging, agricultural films, injection molded products, thermoformed products, and tubes [29]. The tensile strength and glass transition temperature of the BP increased significantly when infused with rice husk based silica [14]. It is known that blending of PLA and starch in adequate proportions enhanced the performance of the polymers [30,31]. The interdependence of starch and PLA can be improved by lowering the starch content [32]. Hence, in order to enhance the properties of BP, additional PLA (25%) is added to develop BPB blend such that the starch content gets lowered to 17%.

In this study, CCSP serves as a filler for BP blended with polylactic acid (PLA) to create biodegradable and recyclable nanocomposite filaments. The carbon nano-powder is dispersed into the polymer matrix by solution blending with chloroform as the solvent. Methanol is added to the solution to produce a precipitate of the composite which is then filtered and dried to extrude 3D printable filaments. The extruded filaments were tested for tensile, DSC, TGA, and electrical conductivity tests to determine the mechanical, thermal, and electrical properties suitable for 3D printing application.

2. Experimentation

2.1. Materials

Polylactic acid (IngeoTM biopolymer 3051D) was purchased from Nature Works LLC, Minnetonka, MN, USA. This polymer was blended with BIOPLAST GF 106/02 (potato starch) purchased from (Biotec® Emmerich am Rhein, Germany). The coconut shell powder sample (particle size of 150 μm) was received from Essentium Materials LLC, a Texas based company, USA. This powder was used to synthesize carbon coconut shell powder (CCSP) as it served as a filler for the polymer matrix.

Chloroform (CHCl $_3$, \geq 99%) was used to dissolve the polymers with the nano-powder in order to create well-dispersed composites. HPLC grade methanol (CH $_3$ OH, \geq 99.9%) was used to precipitate the polymer composites from the chloroform through methanolysis. Both solvents were purchased from Sigma-Aldrich Inc.

2.2. Synthesis of carbon nanoparticles

Autogenic pyrolysis is energy efficient and is eco-friendly method as it prevents the generation of residual waste chemicals [14]. Furthermore, it also requires low temperatures compared to the conventional process. Hence, autogenic pyrolysis is adopted to synthesize the carbon from coconut shell powder. The carbon was synthesized by adding approximately 30 g of coconut shell powder (CSP) into a custom-built MTI autogenic high temperature/pressure reactor. The powder was heated at a rate of 5 °C/min from room temperature to 800 °C and was held isothermally at 800 °C for 2 h without application of pressure. Thus collected carbon was ball milled using a vibratory ball mill, 8000D mixer/mill from SPEX SamplePrep, with Zirconia vials and balls. Two separate zirconia ceramic vials of 45 ml (6.35 cm diameter, 6.8 cm long), each with two zirconia balls (12.7 mm diameter) were loaded with CCSP precursor. Then the ball mill was allowed to run for 10 h. The powder was then separated carefully and then, dried, stored and labeled as CCSP10.

2.3. Characterization of carbon nanoparticles

2.3.1. X-ray diffraction

X-ray diffraction (XRD) analysis was carried out using Rigaku DMAX 2200 diffractometer with monochromatic Cu K γ radiation ($\gamma = 0.154056$ nm) at 40 kV, 30 mA, and 1.2 kW. The diffraction data for the carbon coconut shell powder sample was collected in the 2 θ range (10° – 80°) at a scan rate of 2° /min.

2.3.2. Raman analysis

Raman spectrometry was carried out using Thermo-Scientific DXR Raman spectroscopy to observe the graphitization degree of the carbon coconut shell powder. The laser of the instrument had an excitation wavelength of 785 nm. The range of the spectrum was $0-2500~{\rm cm}^{-1}$ using the laser power of 5.0 mW.

2.3.3. Microscopy

The microstructure of the synthesized carbon coconut shell powder was investigated using JEOL JSM-7200F field emission scanning electron microscope (FESEM, JEOL USA, Peabody, MA) at 10 and 15 kV. The samples were sputter coated with gold/palladium (Au/Pd) for 3 min at 10 mA using Hummer sputter coater.

For transmission electron microscopy (TEM), a JOEL 2010 TEM was used. Carbon nano-powder was first dispersed in ethanol and then dispensed on Cu grid and air dried. TEM analysis was conducted at an operating voltage of 200 kV.

Table 1 Description of the specimens.

Specimen	Description	
BP	BIOPLAST GF 106/02	
BPB	75% of BP and 25% of PLA blend	
BPB-CCSP 0.2 wt%	BPB with 0.2 wt% of CCSP10	
BPB-CCSP 0.6 wt%	BPB with 0.6 wt% of CCSP10	
BPB-CCSP 1 wt%	BPB with 1 wt% of CCSP10	

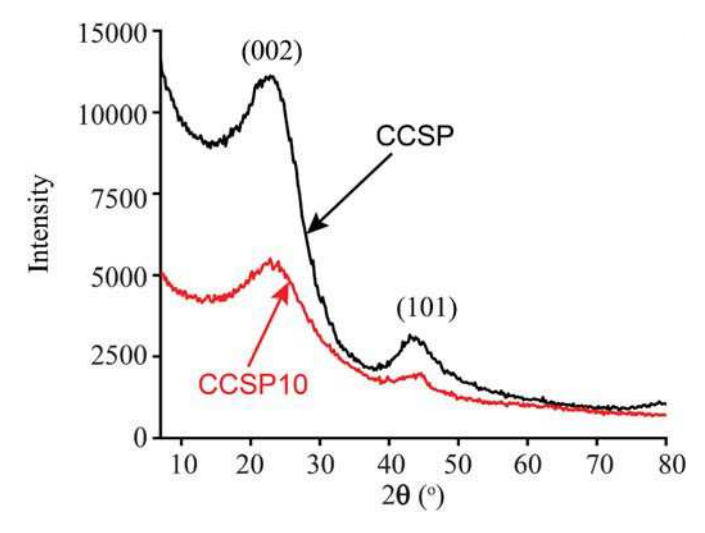


Fig. 1. X-ray diffraction pattern of pre-ballmilled coconut shell powder (CCSP) and coconut shell powder ball milled for 10hrs (CCSP10).

2.4. Development of nanocomposite

The polymer pellets (75% BP and 25% PLA) were dissolved in chloroform. The carbon nano-powder was infused into the polymer solution and this solution is stirred using magnetic stirrer 12 h to obtain uniform dispersion. Mechanical stirring was applied to further dissolve the material. Methanol was added into the solution in order to create a precipitate of the polymer composite. The material was then filtered and dried in a vacuum oven overnight. The powder was then crushed with a pestle and mortar for extrusion. The composite powder was then fed into the EX2 Fil-a-Bot extruder (VT, USA) to extrude filament composites. Extrusion temperature for PLA was 169 °C, 120 °C for BP, and 155 °C for blended systems which resulted in filaments with a diameter of 1.5–1.75 mm. The description of the samples that were developed is summarized in Table 1.

2.5. Characterization of nanocomposites

2.5.1. Thermogravimetric analysis

Thermogravimetric analysis (TGA) was carried out using a TA Q500 TGA to record temperature, mass, first derivative and heat flow of the specimens. The samples were heated up from 30 $^{\circ}\text{C}$ to 500 $^{\circ}\text{C}$ at a heating rate of 10 $^{\circ}\text{C/min}$ under nitrogen gas.

2.5.2. Differential scanning calorimetry

Differential scanning calorimetry (DSC), a TA Q2000, was used to study the thermal behavior of the biodegradable composite. Samples of approximately 12 mg weight were placed in an aluminum pan and was heated from 30 $^{\circ}\text{C}$ to 350 $^{\circ}\text{C}$ at a heating rate of 5 $^{\circ}\text{C/min}.$

2.5.3. Tensile test

A Zwick/Roell Z2.5 Universal Mechanical Testing-Machine with 2.5 kN load cell was used to determine the mechanical properties of the filaments. The composite filaments underwent tensile testing following

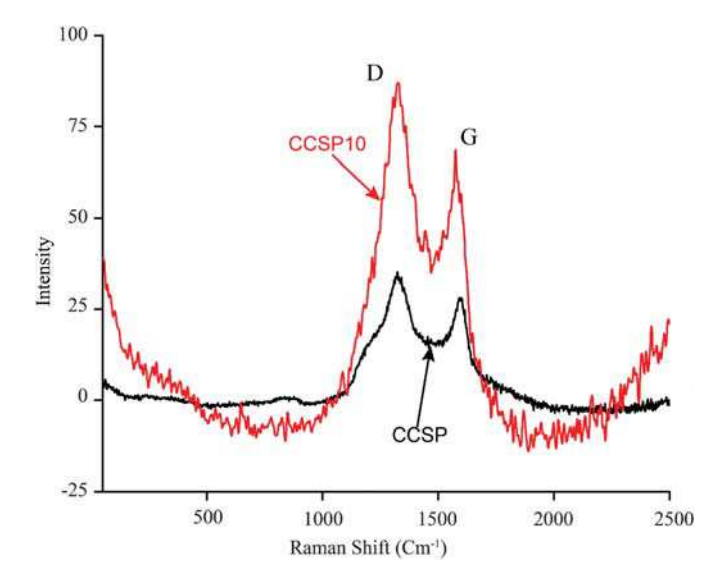


Fig. 2. Raman spectrometry of pre-ball milled coconut shell powder (CCSP) and coconut shell powder ball milled for 10hrs (CCSP10).

ASTM D3379 standard. The testing conditions for the filaments were as follows: gage length was 50 mm, the pre-load tension was 0.1 N, pre-load speed was 0.5 mm, and test speed was 0.5 mm/min. The tensile properties elongation at break and tensile strength were obtained with TestXpert data acquisition and analysis software. The tensile modulus was calculated from the slope of the linear portion of the acquired stress-strain curves using Origin software. Five specimens were tested for each polymer composite system and the average results were considered.

2.5.4. Electrical conductivity test

Electrical conductivity tests were carried out using a 4-point probe by Jandel Model RM3000 version 2.0 with the needle load of the probe set to \leq 50 g. These parameters were applied in order to study the electrical properties of the composites concerning the filler content.

3. Results and discussion

3.1. XRD analysis

The morphology of carbon obtained from the coconut shell powder obtained before (CCSP) and after (CCSP10) ball milling was analyzed using X-Ray diffraction shown in Fig. 1. The data is processed using the standard Joint Committee on Powder Diffraction Standard (JCPDS) card file 41–1487, which is normal graphite-2H with characteristic peaks at 26.38° (002 plane) and 44.39° (101 plane) [33]. The pre-ballmilled carbon exhibits two peaks at 20 of \sim 23° and 44.5° corresponding to the (002) and (101) graphite planes, respectively [15,34]. Similar results were observed by Arsyad *et al.* [20] when activated carbon is produced from coconut shells. The amorphous structure of the carbon is verified from the XRD pattern [20]. No sharp peaks were observed in the pattern which suggests that the carbon obtained from the pyrolysis is amorphous and favors the adsorption [34,35].

Ball milling is an efficient technique to reduce the particle size. The collisions between the ball-to-ball and ball-to-wall results in the breakdown of particles to smaller sizes. Hence, the carbon obtained from the coconut shell powder is ball milled for 10hrs to reduce the particle size. The peaks were observed at 23° and 44.6° which do not have any significant change compared to CCSP. However, the particle size reduction is evident from the XRD pattern of CCSP10 where the peaks corresponding to (002) and (101) planes were broadened.

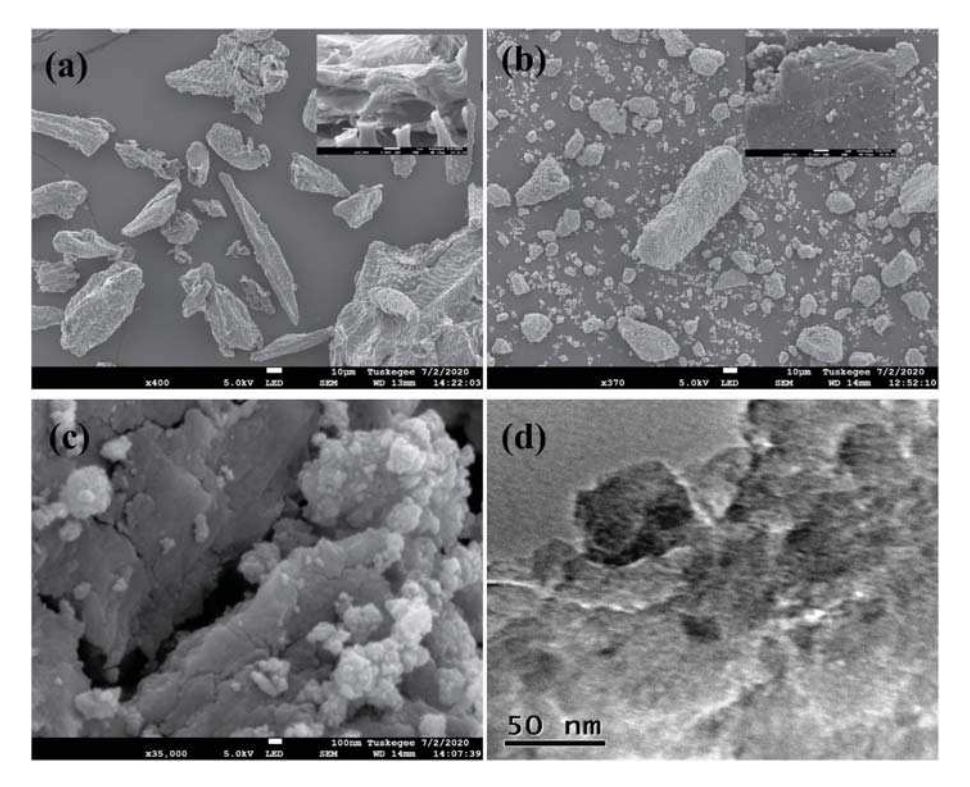


Fig. 3. (a) SEM micrograph of CCSP (pre-ballmilled), (b) CCSP10 (ball milled for 10hrs), (c) magnified view of CCSP10 and (d) TEM micrograph of CCSP10.

3.2. Raman analysis

Raman spectrometry is performed to analyze and verify the presence of carbon as well as its degree of graphitization. Fig. 2 shows the Raman analysis of pre-ballmilled (CCSP) and ball milled coconut shell powder (CCSP10). The intensity of the spectra increased for CCSP10 suggesting the decrease in the particle size. The typical disordered D band peak for pre-ballmilled coconut shell powder is observed at 1323.7 cm⁻¹ and G band is exhibited at 1598.5 cm⁻¹. For the disordered graphite, the Raman analysis shows two characteristic peaks, G peak around 1580–1600 cm⁻¹ and D peak around 1350 cm⁻¹ [36]. Hence, the D and G bands present in CCSP suggest polyaromatic hydrocarbons and graphitic carbon [15]. The D band arises from the defects in the graphitic structure which might be due to the disruption of sp² bands, vacancies etc. whereas G mode arises due to the inplane stretching motion of sp² hybridized carbon atoms [37,38]. The ID/IG ratio for the CCSP was 1.26, where ID and IG correspond to the intensities of D band and G band, respectively. A broad D band peak was observed for CCSP 10 at 1323.5 cm^{-1} and a sharp G band peak at 1576.2 cm^{-1} with ID/IG ratio of 1.28. Although there is no much variation with the D band peak

wavenumbers for preball milled and ball milled coconut shell powder, the G peak moves to the lower wavenumber. This may be due to the strain induced in the particles due to the ball milling, which might have caused damage to the graphitic structure and thus inducing the defects which is evident from the increase in ID/IG ratio [39–41]. In addition, the ball milling also causes the diminishment of the D peak for CCSP10 which suggests that the compressive strain might have been induced during the ball milling process [42]. The peaks present in both CCSP and CCSP10, and the peaks observed in XRD at 23° and 44° suggest that there may be a formation of very small crystallites of graphene-oxide within the coconut shell powder [43]. Furthermore, the increase in ID/IG ratio suggests the decrease of defects in graphene-oxide which has significant sp³ content [36,44]. Under such conditions, the material may possess electrical properties that can enhance the polymer conducting performance when CCSP10 is used as filler [45].

3.3. Surface morphology of carbon nano-powder

The microstructure of coconut shell powder after undergoing pyrolysis is shown in Fig. 3. The carbon from coconut shell powder before

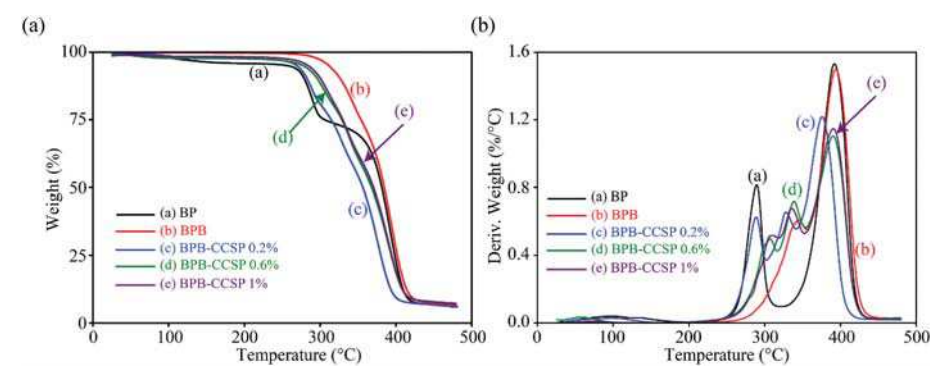


Fig. 4. TGA of the BPB-CCSP blend composites (a) weight and (b) derivative weight.

Table 2 Summary of thermogravimetric analysis.

Specimen	Decomposition temperatures			Residue
	first degradation (°C)	second degradation (°C)	major degradation (°C)	left (%)
BP	289.32	_	392.94	5.9
BPB	344.65	_	394.21	6.6
BPB-CCSP 0.2%	288.66	326.98	376.77	5.7
BPB-CCSP 0.6%	306.82	337.69	391.48	7.1
BPB-CCSP 1%	309.97	335.88	392.34	7.2

Table 3Weight change of composite systems from TGA.

Temperature Range (°C)	BP	BPB	BPB-CCSP 0.2%	BPB-CCSP 0.6%	BPB-CCSP 1%
0–150	3.34	0.14	2.15	1.59	0.36
150–300	20.27	2.57	16.99	9.15	8.01
300–450	69.42	89.86	74.08	80.79	82.6

ball mill treatment (CCSP) contains irregular shapes and chunks as shown in Fig. 3(a). The magnified view in Fig. 3(a) clearly shows the sheet structures of the carbon particles. Fig. 3(b) shows the same powder after receiving 10 h of ball milling treatment. The particles have become less irregular and more of an even shape with decrease in particle size. It is observed that the sheet structures are damaged after ball milling (Fig. 3(b)) which is also evident from the Raman spectrometry. The magnified view of the same carbon powder is shown in Fig. 3(c) which shows spherical nanoparticle clusters in powder that have a size of about $0.5\text{--}7~\mu m$ and the nano-powder itself ranging from 43 to 87 nm. Ball milling for longer duration decreases the particles size and gives the powder a smoother structure when compared to pre-ball mill treated carbon. The decrease in the particle size to nano range is further confirmed by TEM micrograph as shown in Fig. 3(d). The TEM micrographs suggest that the particle size is less than nanometer range. Although most of the particles appear to be irregular in shape, slightly sheet like structures were observed.

3.4. Thermal analysis

The thermal properties of the blended composites were evaluated by TGA and DSC. The TGA curves were shown in Fig. 4. The blended composites have high thermal stability compared to that of the BP. The first, second and major degradation temperatures and the residues of the composite systems are evaluated and summarized in Table 2. All the systems have shown weight loss of around 0.1-3% below 150 °C which might be due to the presence of moisture content. The weight loss of the composite systems in three stages of temperature is summarized in Table 3. The BP has shown two significant transitions as shown in Fig. 4 (a) and (b). The first significant degradation is observed at 289 °C which corresponds to the PLA content present in the BP polymer [14,46]. The second degradation is the major degradation realized at 393 °C which corresponds to the bio-based content (starch) present in the BP [14,46]. This bio-based content is responsible for thermal stability and the toughness of the polymer. The BPB system has shown significant improvement (19%) in first degradation temperature and a small improvement in major degradation temperature which is due to the supplemental PLA present in the blend. In general, starch and PLA are thermodynamically immiscible exhibit distinct thermal decomposition characteristics [31]. In BPB system, when PLA is blended with BP, the starch content decreases from 23% to 17%. As such, the increase in first degradation temperature and the reduction in the distance between two

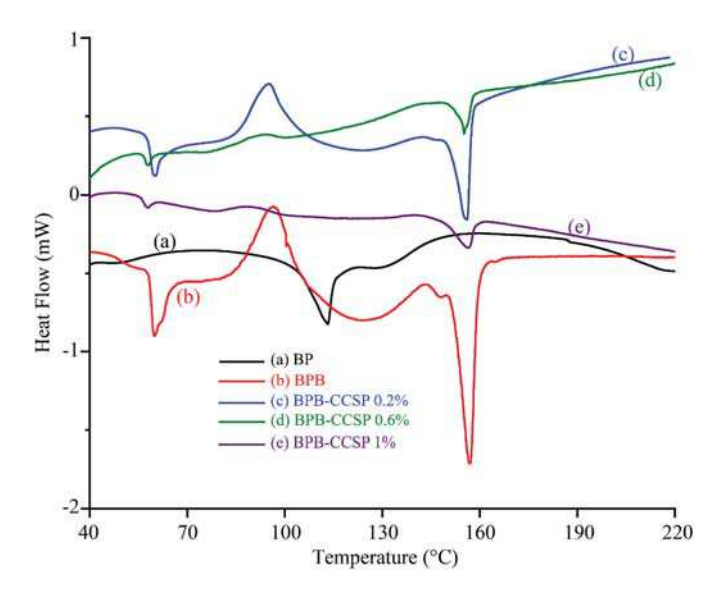


Fig. 5. DSC thermographs of the BPB-CCSP blend composites.

peaks suggest the improved interdependence between the PLA and bio-based content [32].

The onset temperatures for the BPB-CCSP systems slightly decreased compared to that of BPB system. The CCSP nanoparticles infused in the BPB system have resulted in four step decomposition whereas BP and BPB have resulted in three step degradation process where the first decomposition corresponds to the moisture content. Similar results were observed for Poly Vinyl Alcohol (PVA)/starch/biochar composites, when the biochar is infused into PVA/starch blend [47] implying that biochar quickly breakdown the PVA/starch matrix resulting in early degradation. The second and third steps which are observed between 250° and 350° C might be due to the degradation of backbone cleavage and side chains of polymer matrix [47]. It is anticipated that infusing CCSP nanoparticles into BPB will result in higher thermal stability. However, the infused CCSP nanoparticles decreased the thermal stability of PLA content which can be attributed to the presence of large amount of PLA and tiny amounts of CCSP [48]. Furthermore similar results were observed by Arrigo et al. [12] suggesting that the potassium content present in the biochar leads to the detrimental effect of thermal stability of PLA. The CCSP nanoparticles have slightly lowered the degradation temperatures between 327°C and 336 °C compared to the maximum degradation temperature of the PLA content in BPB system which is 345 °C. The degradation due to the starch content does not exhibit significant change due to the presence of CCSP nanoparticles. The bio-based content of the BP might have acted as plasticizer preventing the physical crosslinking between the BPB system and carbon nanoparticles [49]. Nevertheless, the developed composite filaments can remain stable and are suitable for applications within the temperature range of 30°-250 °C relevant to neat PLA without venturing any thermal degradation [48,50].

The weight change of BPB-CCSP systems was lower than BP in the range of $150^{\circ}\text{C}-300^{\circ}\text{C}$ and was higher than BP after 300°C . Between $150^{\circ}\text{-}300^{\circ}\text{C}$, the CCSP nanoparticles induced the early degradation of the polymer matrix thus resulting in higher weight change compared to the BPB system. Above 300°C , in addition to the part of the PLA content present in the BPB-CCSP blend, the starch content also degraded resulting in the weight change as observed in Table 3. The BPB-CCSP composites with 0.6 wt% and 1 wt% yielded higher residues compared to the BP and BPB systems which might be due to the high thermal stability of carbon nanoparticles [48]. The resulting behavior might be due to the effective dispersion of carbon particles into the matrix. The increase in the residue percentages for 0.6 wt% and 1% filler loadings suggest that the carbon particles hinder the reactive chemical

C.O. Umerah et al. Composites Part B 202 (2020) 108428

 Table 4

 Summary of differential scanning calorimetry analysis.

Specimen	Glass transition temperature T_g (°C)	Melting temperature T _m (°C)	Melting enthalpy (J/g)	Cold crystallization temperature T_{cc} (°C)
BP	54	113.22	6.0	97.98
BPB	59.2	157.13	6.68	96.54
BPB-CCSP 0.2%	58.9	156.17	6.04	95.14
BPB-CCSP 0.6%	57.25	155.20	6.62	93.10
BPB-CCSP 1%	56.55	156.13	6.48	89.26

groups and subside the weight loss of the polymer composite [17]. Thus, the infusion of the CCSP nanoparticles is inherently beneficial when the amount of residue is the major concern [13,48].

The thermal stability of the BPB-CCSP composite blended systems was further examined by DSC analysis and the results were shown in Fig. 5. The glass transition temperature (Tg) of the BP is observed at 54 °C which agrees with the T_g reported by Imam et al. [14] and the melting temperature (T_m) was observed at 113 °C. The BP when blended with PLA exhibited significant increase in the T_m from 113 $^{\circ}\text{C}$ to 157 $^{\circ}\text{C}$ (Table 4) which corresponds to the melting temperature of PLA. In addition to that, T_g also improved to 58 °C with the addition of PLA and reduction in starch content in BPB system [32]. The thermograms exhibited by BPB and BPB-CCSP composites were different from that of BP. However, no significant change was observed either in T_g or T_m with the presence of CCSP at various filler loading percentages. However, Tg and T_m of the BPB-CCSP composites were higher compared to that of BP. The sharp peaks related to Tg and Tm in BPB (Fig. 5 curve (b)) becomes indistinct with the increase in CCSP loading. Similar behavior was observed for biochar loaded polypropylene composites suggesting that less energy would be required for crystallization [13]. The Tg slightly decreased for BPB-CCSP composites compared to the BPB system but were higher than the BP. This can be attributed to the enhanced mobility of the PLA molecules which is observed from the degradation phenomena in TGA [12]. The T_m of BPB-CCSP composites does not exhibit any significant shift compared to BPB system [13]. The melting enthalpy for all the blend systems is higher than the BP suggesting that there is no physical crosslinking due to the interaction of the carbon particles present with the polymer. The interfacial bonding between the polymer and nanoparticles might be extremely weak as the bio-based content acts as plasticizer. Due to the lack of availability of data on the crystallinity of BP, the crystallinity of the blended systems was not evaluated. The cold crystallization temperatures (T_{cc}) decreased significantly with the addition of PLA as well as CCSP suggesting that the CCSP particles act as nucleating agents accelerating the crystallization of the blended composites [15]. The movement of the long polymer chain segments might have been impeded by the CCSP particles such that these polymer chains can be arranged in order with the CCSP particles promoting the crystallization at low temperatures [14]. Furthermore, the increase in the CCSP loading resulted in the complete crystallization of the composites which is observed from the diminishment of shoulder peaks for melting endotherms. The overall thermal behavior of the polymer composites is influenced by the bio-based content present in the BP as well as the dispersion of the carbon nanoparticles in the matrix.

3.5. Mechanical analysis

The mechanical properties of the extruded composite systems were analyzed using a tensile test. The tensile behavior and properties of the extruded filaments were shown in Fig. 6 and were summarized in Table 5. In the initial stages, all the systems have toe region which corresponds to the adjustment of the filament in the grips of the tensile test equipment. Hence, the Young's modulus is calculated from the slope of the linear portion in the graph by using Origin software. The BPB-CCSP systems exhibit high strength and modulus compared to BP (Fig. 6(a) and (b)). However, due to the presence of bio-based content, BP exhibits highest strain of 1.77% at maximum force (F_{max}). The addition of PLA (BPB) contributes to the enhancement in strength and modulus but do not exhibit any significant change for the strain at maximum force F_{max}. The addition of CCSP to the system significantly influenced the mechanical behavior of the filaments. The tensile strength and modulus were higher for the BPB-CCSP systems compared to the BP and BPB. The BPB-CCSP composite system with 0.6 wt% loading has shown highest tensile strength (16.12 MPa) and modulus (3.54 GPa) which were increased by 80% and 5%, respectively compared to BP. The strain at F_{max} decreased due to the presence of carbon which is expected because the bio-based content in BP prohibits the crosslinking of the particles with the polymer chain. Hence, the mechanical behavior owes to the homogenous dispersion of CCSP in polymer [12]. As the filler loading increases to 1 wt% the tensile properties starts to deteriorate to the agglomeration of nanoparticles. Despite the ratio of the PLA and starch material, the addition of the

Table 5Summary of tensile properties.

Specimen	Tensile modulus (GPa)	Tensile strength (MPa)	Strain at maximum stress (%)
BP	0.58 ± 0.04	8.9 ± 0.53	1.77 ± 0.06
BPB	0.84 ± 0.04	10.58 ± 0.3	1.75 ± 0.03
BPB-CCSP 0.2%	2.69 ± 0.23	12.33 ± 0.01	0.73 ± 0.01
BPB-CCSP 0.6%	3.54 ± 0.11	16.19 ± 0.31	0.61 ± 0.07
BPB-CCSP 1%	2.75 ± 0.19	13.86 ± 0.46	0.62 ± 0.02

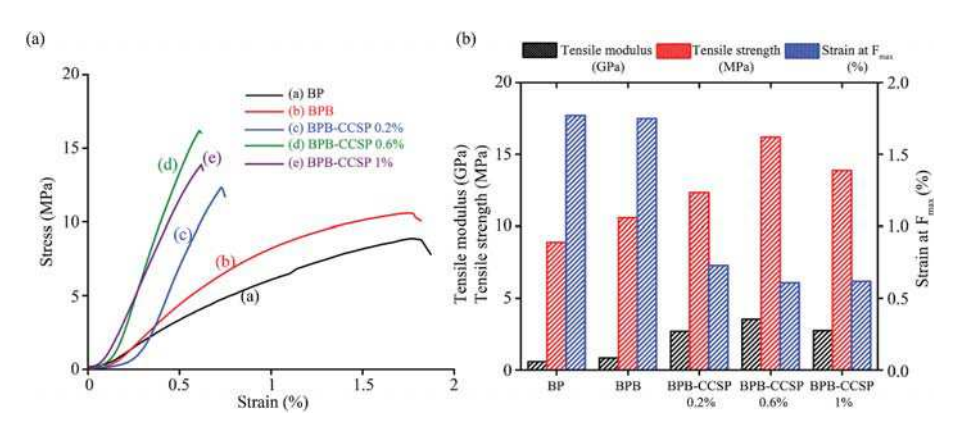


Fig. 6. (a) Stress-strain behavior and (b) tensile properties of BPB-CCSP composites.

C.O. Umerah et al.

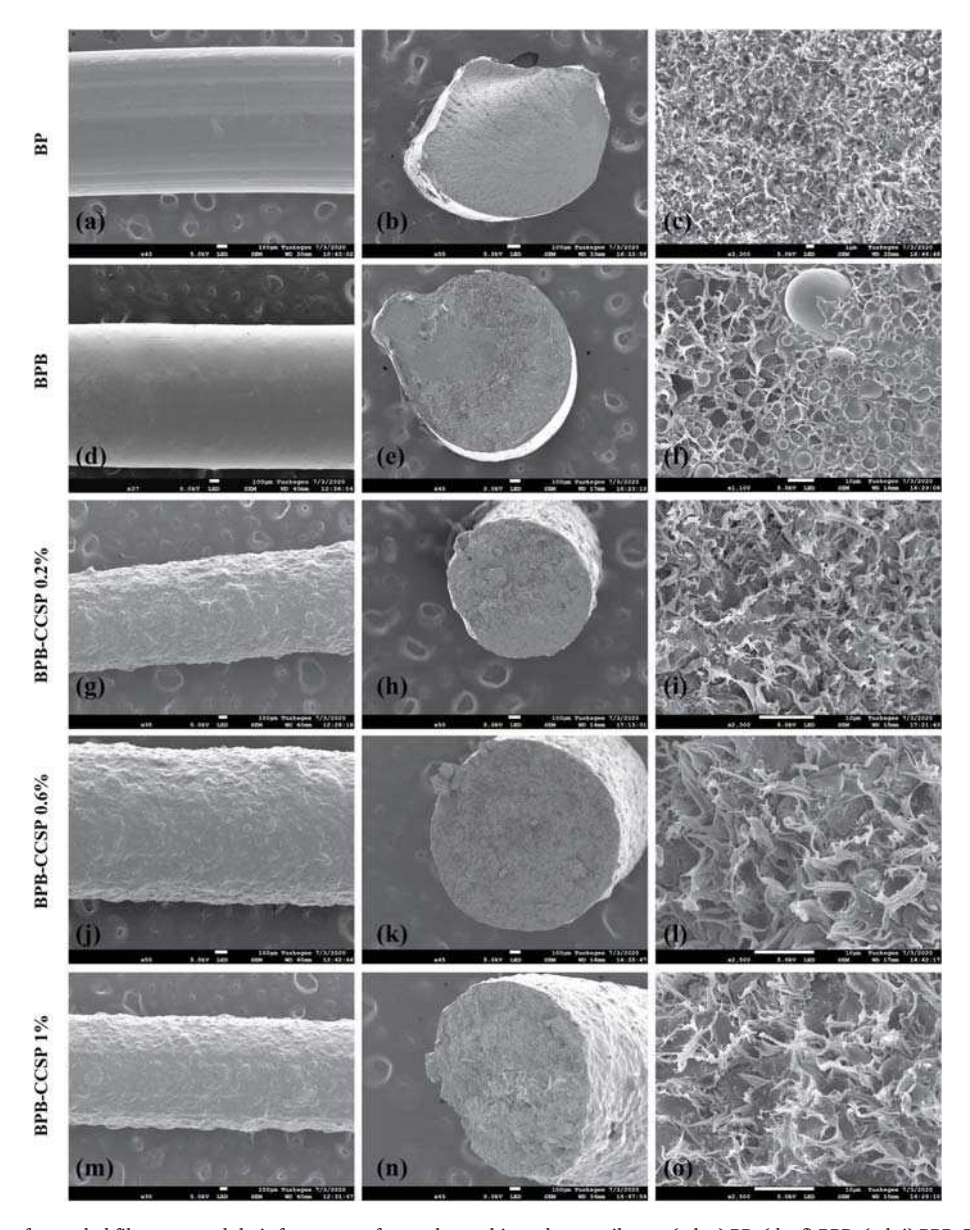


Fig. 7. SEM micrographs of extruded filaments and their fracture surfaces when subjected to tensile test (a,b,c) BP, (d,e,f) BPB, (g,h,i) BPB-CCSP 0.2 wt%, (j,k,l) BPB-CCSP 0.6 wt% and (m,n,o) BPB-CCSP 1 wt%.

carbon particles even at low percentages have improved the strength of the composites compared to the results of Eaysmine et al. [30] and Sanyang et al. [51].

The morphology of the surfaces of the extruded filaments and their fracture surfaces when subjected to tensile tests for BP and BPB composite blend systems were shown in Fig. 7. The surface of the BP filament is smooth without any irregularities as shown in Fig. 7(a). The striations due to extrusion were seen on the surface of BP. The fracture surface of the bio-based BP is disoriented as BP is a soft polymer (Fig. 7(b)). The fracture surface shows the mixture of polymer and starch blend without any unevenness (Fig. 7(c)). The BPB filament is smooth without any unevenness. However, the color differences on the filament surface suggest the poor miscibility of PLA in BP (Fig. 7(d)). This is further confirmed by the fracture surfaces which show smooth and rough surfaces (Fig. 7(e) and (f)). The PLA when blended with BP fills the voids first and then gets assorted in the blend. Hence, two different structures were seen in BPB fracture surface (Fig. 7(f)). The BPB-CCSP composites exhibit the presence of carbon and the fracture planes suggest that the filaments did not undergo any necking and were less ductile (Fig. 7(g),

(j) and (m)). The fracture surface of BPB-CCSP 0.2% also reveals the presence of carbon and the surface is uniform with the blend of BPB and carbon (Fig. 7(h) and (i)). The BPB-CCSP composite with 0.6 wt% carbon which exhibited high tensile strength and modulus were shown in Fig. 7(k) and (l). The surface noticeably indicates the increase in the presence of carbon compared to BPB-CCSP 0.2%. Furthermore, the surface does not exhibit any voids which suggest the effective dispersion of particles and thus demonstrated high tensile strength. As the carbon content increases, the carbon particles agglomerates and result in the downturn of tensile properties (Fig. 7(n) and (o)). The fracture happens at the agglomeration site as shown in Fig. 7(n). Furthermore, the increased carbon content also results in voids which cause the decrement of strength (Fig. 7(o)). Thus the carbon from the coconut shell powder, when infused in moderate quantities with effective dispersion improves the mechanical properties of the polymer. Since these filaments are aimed for future 3D printing applications we have tested the basic printability of the filament which is shown in supplementary material. However, the analysis of 3D printed parts is left for future

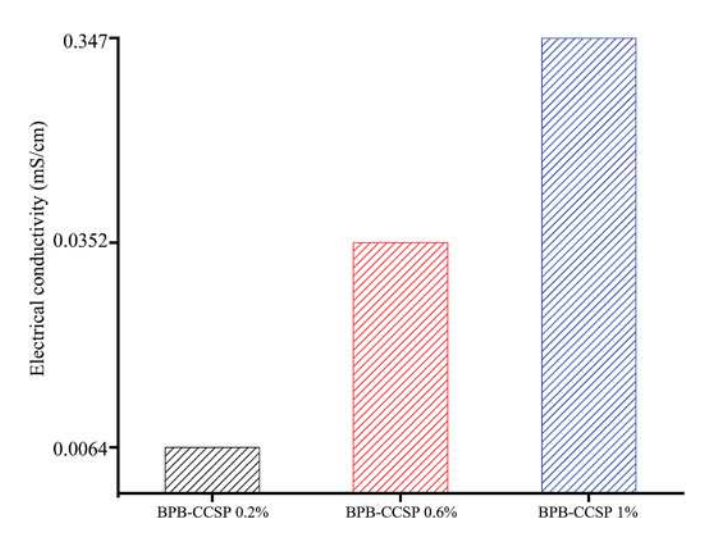


Fig. 8. Electrical conductivity of BPB-CCSP blend composites at 0.2, 0.6 and 1 wt% loading.

3.6. Electrical conductivity test

The electrical conductivity of BPB-CCSP nanocomposites was tested and is shown in Fig. 8. The electrical conductivity of the filaments was analyzed using 4-point probe by Jandel Model RM3000 Version 2.0. The values observed for the electrical conductivity are very low. As the filler loading increases, the electrical conductivity values also increased. Despite low electrical conductivity, it can be inferred that the presence of carbon particles revealed the electrical properties of the extruded filaments. This provides the scope for future work to enhance the electrical conductivity of these composites by modifying the structure of carbon and by increasing the filler content.

4. Conclusions

The biodegradable polymer nanocomposites using a carbon-based filler from coconut shell powder were successfully developed and investigated. Carbon extracted from the coconut shell powder serves as filler material for the polymer and enhances the mechanical properties of blended composites. The thermal and mechanical properties were improved with addition of PLA and CCSP to the BP. Although there is no much significant improvement in thermal properties of BPB-CCSP composites compared to BPB, the trends exhibited by TGA and DSC were noteworthy with the additional decomposition and reduced cold crystallization temperatures. The mechanical properties were significantly improved with the addition of CCSP particles with effective dispersion. However, high filler percentages lead to the agglomeration of particles which deteriorates the performance of the filaments. Although not substantial, the electrical conductivity of the filaments was improved with the increase in filler percentages. Preparation of highly crystalline carbon from coconut shell powder and further improving the thermal, mechanical and electrical properties was left for future work. The extruded BPB-CCSP composites can be used as an alternative for polymers like low-density polyethylene (LDPE) due to high tensile strength. The results suggest that extruded samples can create polymer nanocomposites with high mechanical, thermal, and electrical properties that can be potentially used for 3D printing, biomedical and food packaging applications.

Declaration of competing interest

The authors declare that they have no known competing financial interests or personal relationships that could have appeared to influence the work reported in this paper.

Acknowledgements

The authors would like to acknowledge the financial support of NSF-RISE #1459007 NSF-CREST#1735971, Al-EPSCoR#1655280, and NSF-MRI-1531934.

Appendix A. Supplementary data

Supplementary data to this article can be found online at https://doi. org/10.1016/j.compositesb.2020.108428.

References

- [1] Polamaplly P, Cheng Y, Shi X, Manikandan K, Zhang X, Kremer GE, et al. 3D printing and characterization of hydroxypropyl methylcellulose and methylcellulose for biodegradable support structures. Polymer 2019;173:119–26. https://doi.org/10.1016/j.polymer.2019.04.013.
- [2] Sundarababu J, Anandan SS, Griskevicius P. Evaluation of mechanical properties of biodegradable coconut shell/rice husk Powder polymer composites for light weight applications. Mater Today Proc 2020. https://doi.org/10.1016/j. matpr.2020.04.095.
- [3] Wu CS, Liao HT, Cai YX. Characterisation, biodegradability and application of palm fibre-reinforced polyhydroxyalkanoate composites. Polym Degrad Stabil 2017;140: 55–63. https://doi.org/10.1016/j.polymdegradstab.2017.04.016.
- [4] Sharma R, Singh R, Penna R, Fraternali F. Investigations for mechanical properties of Hap, PVC and PP based 3D porous structures obtained through biocompatible FDM filaments. Compos B Eng 2018;132:237–43. https://doi.org/10.1016/j. compositesb.2017.08.021.
- [5] Guo Y, Chang CC, Cuiffo MA, Xue Y, Zuo X, Pack S, et al. Engineering flame retardant biodegradable polymer nanocomposites and their application in 3D printing. Polym Degrad Stabil 2017;137:205–15. https://doi.org/10.1016/j. polymdegradstab.2017.01.019.
- [6] Pakkanen J, Manfredi D, Minetola P, Iuliano L. About the use of recycled or biodegradable filaments for sustainability of 3D printing. In: Campana G, Howlett RJ, Setchi R, Cimatti B, editors. Sustain. Des. Manuf. Cham: Springer International Publishing; 2017. p. 776–85.
- [7] Udhayasankar R, Karthikeyan B. A review on coconut shell reinforced composites. Int J Chem Res 2015;8:624–37.
- [8] Filgueira D, Holmen S, Melbø JK, Moldes D, Echtermeyer AT, Chinga-Carrasco G. 3D printable filaments made of biobased polyethylene biocomposites. Polymers 2018;10. https://doi.org/10.3390/polym10030314.
- [9] Wang X, Jiang M, Zhou Z, Gou J, Hui D. 3D printing of polymer matrix composites: a review and prospective. Compos B Eng 2017;110:442–58. https://doi.org/ 10.1016/j.compositesb.2016.11.034.
- [10] Mohanty AK, Vivekanandhan S, Pin JM, Misra M. Composites from renewable and sustainable resources: challenges and innovations. Science 2018;362:536–42. https://doi.org/10.1126/science.aat9072. 80-.
- [11] Bourmaud A, Beaugrand J, Shah DU, Placet V, Baley C. Towards the design of high-performance plant fibre composites. Prog Mater Sci 2018;97:347–408. https://doi.org/10.1016/j.pmatsci.2018.05.005.
- [12] Arrigo R, Bartoli M, Malucelli G. Polymers poly (lactic acid) biochar Biocomposites: effect of processing and filler content on rheological, thermal and mechanical properties. Polymers 2020;12:1–13.
- [13] Das O, Bhattacharyya D, Hui D, Lau K-T. Mechanical and flammability characterisations of biochar/polypropylene biocomposites. Compos B Eng 2016; 106:120–8. https://doi.org/10.1016/j.compositesb.2016.09.020.
- [14] Imam MA, Jeelani S, Rangari VK. Thermal decomposition and mechanical characterization of poly (lactic acid) and potato starch blend reinforced with biowaste SiO2. J Compos Mater 2019;53:2315–34. https://doi.org/10.1177/ 0021998319826377.
- [15] Idrees M, Jeelani S, Rangari V. Three-dimensional-printed sustainable biocharrecycled PET composites. ACS Sustainable Chem Eng 2018;6. https://doi.org/ 10.1021/acssuschemeng.8b02283. 13940–8.
- [16] Li S, Li X, Chen C, Wang H, Deng Q, Gong M, et al. Development of electrically conductive nano bamboo charcoal/ultra-high molecular weight polyethylene composites with a segregated network. Compos Sci Technol 2016;132:31–7. https://doi.org/10.1016/j.compscitech.2016.06.010.
- [17] Ho MP, Lau KT, Wang H, Hui D. Improvement on the properties of polylactic acid (PLA) using bamboo charcoal particles. Compos B Eng 2015;81:14–25. https://doi. org/10.1016/j.compositesb.2015.05.048.
- [18] Mas'udah KW, Nugraha IMA, Abidin S, Mufid A, Astuti F, Darminto. Solution of reduced graphene oxide synthesized from coconut shells and its optical properties. AIP Conf Proc 2016;1725. https://doi.org/10.1063/1.4945499.
- [19] Kishore Chowdari G, Krishna Prasad DVV, Devireddy SBR. Physical and thermal behaviour of areca and coconut shell powder reinforced epoxy composites. Mater Today Proc 2020;2–5. https://doi.org/10.1016/j.matpr.2020.02.282.
- [20] Arsyad NAS, Razab MKAA, Noor AM, Amini MH, Mohamad, Yusoff NNAN, et al. Effect of chemical treatment on production of activated carbon from Cocos nucifera L. (coconut) shell by microwave irradiation method. J Trop Resour Sustain Sci 2016:4:112-6.
- [21] Ratnoji SS, Singh N. A study of coconut shell activated carbon for filtration and its comparison with sand filtration. Int J Renew Energy Environ Eng 2014:3–6. 02.

- [22] Ramaraj B, Poomalai P. Ecofriendly poly(vinyl alcohol) and coconut shell powder composite films: physico-mechanical, thermal properties, and swelling studies. J Appl Polym Sci 2006;102:3862–7. https://doi.org/10.1002/app.23913.
- [23] Somashekhar TM, Naik P, Nayak V, Mallikappa Rahul S. Study of mechanical properties of coconut shell powder and tamarind shell powder reinforced with epoxy composites. IOP Conf Ser Mater Sci Eng 2018;376. https://doi.org/10.1088/ 1757-899X/376/1/012105.
- [24] Thaker N, Srinivasulu B, Shit SC. A study on characterization and comparison of alkali treated and untreated coconut shell powder reinforced polyester composites. Int J Sci Eng Tech 2013;473:469–73.
- [25] Navaneethakrishnan S, Athijayamani A. Measurement and analysis of thrust force and torque in drilling of sisal fiber polymer composites filled with coconut shell powder. Int J Plast Technol 2016;20:42–56. https://doi.org/10.1007/s12588-016-9139-2.
- [26] Chun KS, Husseinsyah S, Osman H. Mechanical and thermal properties of coconut shell powder filled polylactic acid biocomposites: effects of the filler content and silane coupling agent. J Polym Res 2012;19. https://doi.org/10.1007/s10965-012-0850.8
- [27] Sikora J, Majewski Ł, Puszka A. Modern biodegradable plastics—processing and properties: Part I. Materials 2020;13:1986. https://doi.org/10.3390/ma13081986
- [28] Babu RP, O'Connor K, Seeram R. Current progress on bio-based polymers and their future trends. Prog Biomater 2013;2:8. https://doi.org/10.1186/2194-0517-2-8.
- [29] Arrow Greentech. BioplastGF106/02. 2019.
- [30] Eaysmine S, Haque P, Ferdous T, Gafur MA, Rahman MM. Potato starch-reinforced poly(vinyl alcohol) and poly(lactic acid) composites for biomedical applications. J Thermoplast Compos Mater 2016;29:1536–53. https://doi.org/10.1177/ 0892705715569824.
- [31] Muller J, González-Martínez C, Chiralt A. Combination of Poly(lactic) acid and starch for biodegradable food packaging. Materials 2017;10:1–22. https://doi.org/ 10.3390/ma10080952.
- [32] Zuo Y, Gu J, Cao J, Wei S, Tan H, Zhang Y. Effect of starch/polylactic acid ratio on the interdependence of two-phase and the properties of composites. J Wuhan Univ Technol -Materials Sci Ed 2015;30:1108–14. https://doi.org/10.1007/s11595-015-1280-9.
- [33] Goni A, Rampe MJ, Kapahang A, Turangan TM. Making and characterization of active carbon from coconut shell charcoal. Int J Adv Educ Res 2019;4:40–3.
- [34] Pechyen C, Atong D, Aht-Ong D, Sricharoenchaikul V. Investigation of pyrolyzed chars from physic nut waste for the preparation of activated carbon. J Solid Mech Mater Eng 2007;1:498–507. https://doi.org/10.1299/jmmp.1.498.
- [35] Das D, Samal DP, Bc M. Preparation of activated carbon from green coconut shell and its characterization. J Chem Eng Process Technol 2015. https://doi.org/ 10.4172/2157-7048.1000248.06.
- [36] Ferrari AC, Roberston J. Interpretation of Raman spectra of disordered and amorphous carbon. Phys Rev B 2000;61. https://doi.org/10.1007/BF02543692.
- [37] Manoj B. Synthesis and characterization of porous, mixed phase, wrinkled, few layer graphene like nanocarbon from charcoal. Russ J Phys Chem 2015;89: 2438–42. https://doi.org/10.1134/S0036024415130257.

- [38] Kurniasari Maulana A, Nugraheni AY, Jayanti DN, Mustofa S, Baqiya MA, et al. Defect and magnetic properties of reduced graphene oxide prepared from old coconut shell. IOP Conf Ser Mater Sci Eng 2017;196. https://doi.org/10.1088/ 1757-899X/196/1/012021.
- [39] Kim JW, Jeong JW, Kang JT, Choi S, Ahn S, Song Y-H. Highly reliable field electron emitters produced from reproducible damage-free carbon nanotube composite pastes with optimal inorganic fillers. Nanotechnology 2014;25. https://doi.org/ 10.1088/0957-4484/25/6/065201.
- [40] Calderón-Ayala G, Cortez-Valadez M, Mani-Gonzalez PG, Hurtado RB, Contreras-Rascón JI, Carrillo-Torres RC, et al. Green synthesis of reduced graphene oxide using ball milling. Carbon Lett 2017;21:93–7. https://doi.org/10.5714/ CL 2017.21.093
- [41] Liang A, Jiang X, Hong X, Jiang Y, Shao Z, Zhu D. Recent developments concerning the dispersion methods and mechanisms of graphene. Coatings 2018;8. https://doi. org/10.3390/coatings8010033.
- [42] Narayana MV, Jammalamadaka SN. Tuning optical properties of graphene oxide under compressive strain using wet ball milling method. Graphene 2016:73–80. https://doi.org/10.4236/graphene.2016.52008. 05.
- [43] Prasetya FA, Nasrullah M, Nugraheni AY, Darminto. Study of Raman spectroscopy on graphene phase from heat treatment of coconut (Cocus Nucifera) shell. Mater Sci Forum 2015;827:290–3. https://doi.org/10.4028/www.scientific.net/MS F.827.290.
- [44] King AAK, Davies BR, Noorbehesht N, Newman P, Church TL, Harris AT, et al. A new Raman metric for the characterisation of graphene oxide and its derivatives. Sci Rep 2016;6:1–6. https://doi.org/10.1038/srep19491.
- [45] Radoń A, Włodarczyk P, Łukowiec D. Structure, temperature and frequency dependent electrical conductivity of oxidized and reduced electrochemically exfoliated graphite. Phys E Low-Dimensional Syst Nanostructures 2018;99:82–90. https://doi.org/10.1016/j.physe.2018.01.025.
- [46] Kopinke FD, Remmler M, Mackenzie K, Möder M, Wachsen O. Thermal decomposition of biodegradable polyesters - II. Poly(lactic acid). Polym Degrad Stabil 1996;53:329–42. https://doi.org/10.1016/0141-3910(96)00102-4.
- [47] Terzioğlu P, Parın FN. Biochar reinforced polyvinyl alcohol/corn starch biocomposites. J Nat Appl Sci 2020;24:35–42. https://doi.org/10.19113/ sdufenbed.568229.
- [48] Nizamuddin S, Jadhav A, Qureshi SS, Baloch HA, Siddiqui MTH, Mubarak NM, et al. Synthesis and characterization of polylactide/rice husk hydrochar composite. Sci Rep 2019;9:1–11. https://doi.org/10.1038/s41598-019-41960-1.
- [49] Hassan TA, Rangari VK, Jeelani S. Value-added biopolymer nanocomposites from waste eggshell-based CaCO 3 nanoparticles as fillers. ACS Sustainable Chem Eng 2014;2:706–17. https://doi.org/10.1021/sc400405v.
- [50] Das K, Ray D, Banerjee I, Bandyopadhyay NR, Sengupta S, Mohanty AK, et al. Crystalline morphology of PLA/clay nanocomposite films and its correlation with other properties. J Appl Polym Sci 2010;118:143–51. https://doi.org/10.1002/ app.32345.
- [51] Sanyang ML, Sapuan SM, Jawaid M, Ishak MR, Sahari J. Development and characterization of sugar palm starch and poly(lactic acid) bilayer films. Carbohydr Polym 2016;146:36–45. https://doi.org/10.1016/j.carbpol.2016.03.051.